

# Linear optical response of a non-collinear textured ferromagnet with Rashba coupling

E. Karashtin<sup>1,2,\*</sup> and G. Tatara<sup>3</sup>

<sup>1</sup>*University of Nizhny Novgorod, 23 Prospekt Gagarina, 603950, Nizhny Novgorod, Russia*

<sup>2</sup>*Institute for Physics of Microstructures RAS, GSP-105, 603950, Nizhny Novgorod, Russia*

<sup>3</sup>*RIKEN Center for Emergent Matter Science (CEMS), 2-1 Hirosawa, Wako, Saitama 351-0198, Japan*  
(Dated: July 18, 2019)

We report a theoretical study of a magneto-optical effect that appears in a non-collinearly magnetized media in the presence of the spin-orbit Rashba coupling. The effect is described by the equilibrium spin current tensor of the non-collinear ferromagnet: the addition of electric polarization is linear with respect to this spin current. The considered effect appears due to transitions of conduction electrons between spin subbands caused by the interplay between the spin texture of a non-collinearly magnetized medium and the Rashba coupling. Depending on the type of magnetization distribution (diagonal or off-diagonal spin current), these transitions give rise to an intensity or polarization effect in optics. We consider two particular examples: magnetic helicoid (spin current is diagonal) and magnetic cycloid (spin current is off-diagonal). In the former case the main effect is polarization rotation, while in the latter case an intensity effect appears. These effects exist in media with zero net magnetization. They could be observed e.g. in reflection of light by a non-collinear magnetic medium.

PACS numbers: 75.30.Et, 75.50.Cc, 75.70.Cn

## I. INTRODUCTION

Magnetic systems with non-uniform, and particularly non-collinear, magnetization distribution attract a lot of attention<sup>1–5</sup>. This is caused by a wide range of phenomena that are allowed in such systems. For instance, magnetization switching by a dc current<sup>6,7</sup> is generally attributed to non-collinear magnetic structure. The spin pumping and spin battery phenomena<sup>8,9</sup> arise from the magnetization that is non-collinear in time. Electric manipulation of non-collinear magnetic states such as domain wall motion<sup>10–17</sup> and topological states such as magnetic skyrmions<sup>18–23</sup> is expected to create new types of data storage with less energy losses.

One of the possibilities of electric manipulation of magnetic moment is connected to the co-existence of magnetic moment and electric polarization in the media. There are some well-known magnetoelectric (Cr<sub>2</sub>O<sub>3</sub><sup>24,25</sup>) and multiferroic (BiFeO<sub>3</sub><sup>26,27</sup> and others<sup>28</sup>) materials where the magnetic order and electric polarization co-exist in different ways. It was shown that non-collinear magnetic system with the magnetization  $\mathbf{M}(\mathbf{r})$  should give rise to a non-linear contribution to the electric polarization  $\mathbf{P}_{\text{me}}$ <sup>28–30</sup>:

$$\mathbf{P}_{\text{me}} \propto (\mathbf{M} \text{div} \mathbf{M} - (\mathbf{M} \cdot \nabla) \mathbf{M}). \quad (1)$$

This flexo-magnetoelectric (determined by magnetization change in space) effect, in turn, leads to another possibility to manipulate the magnetization by electric field<sup>31–33</sup>. The appearance of the electric polarization may be attributed to the existence of spin current in non-collinear magnetic media<sup>34–41</sup>. Indeed, the vector  $\mathbf{P}_{\text{me}}$  may be coupled to the antisymmetric part of the spin current tensor  $J_{ij}^S$  ( $i$  and  $j$  denotes the direction of flow and spin, respectively) as  $P_{\text{me}k} = \epsilon_{ijk} J_{ij}^S$  where  $\epsilon_{ijk}$  is the antisymmetric Levi-Civita tensor (for derivation, see Section II).

Recently it was shown that this spin current provides a mechanism of second harmonic generation when the medium interacts with electromagnetic wave<sup>42–45</sup>. As the spin current tensor changes its sign under spatial inversion operation, it gives rise to the second harmonic polarization determined as  $P_i^{2\omega} = \beta_{ijkmn} J_{jk}^S E_m E_n$ , where  $\beta_{ijkmn}$  is a rank five tensor,  $\mathbf{E}$  is the first harmonic wave electric field. Similar linear response of the medium with spatial dispersion of light was predicted in the framework of hydrodynamic theory<sup>46</sup>. There the polarization is defined as  $P_i = \beta'_{ijkmn} J_{jk}^S q_m E_n$ ,  $\mathbf{q}$  is the wavevector of the electromagnetic wave. The equations that define both these linear and non-linear effects do not obey the exchange coupling symmetry, that is, the invariance with respect to coherent rotation of all magnetization vectors in the system<sup>47</sup>. Therefore the discussed effects utilize spin-orbit interaction that is necessary to convert the spin current into electric polarization.

In the mentioned investigations<sup>44–46</sup> the spin-orbit coupling was taken into account phenomenologically as a spin Hall effect. In this paper, we provide a microscopic theory of linear optical response to the electromagnetic wave in a non-collinear magnetic medium. We take the Rashba coupling<sup>48</sup> as a spin-orbit coupling of quite simple form that allows new optical effects in a non-collinearly magnetized system. We show that the electric polarization induced by the wave electric field in such media with Rashba coupling appears without spatial dispersion of light.

The paper is organized as follows. In Section II we discuss the effects of magnetism on optical response of a system from a symmetry point of view. This analysis allows to show the possibility and main geometric properties of the new effect caused by the spin current. Section III is devoted to our approach to microscopic calculations of the optical response of magnetized medium. The cal-

culations are carried out in the framework of the non-equilibrium Green's functions method<sup>49</sup>. Finally, our results are presented and discussed in Section IV.

## II. SYMMETRY CONSIDERATIONS

In this section we analyze possible magneto-optical effects from a symmetry point of view. We consider a magnetic medium with nonuniform magnetization  $\mathbf{M}(\mathbf{r})$  that is non-collinear in space. The effects that appear due to this important property of the magnetization distribution are the focus of our attention.

Uniform magnetization  $\mathbf{M}$  affects isotropic optical response as a rotation of polarization of light, known as the Faraday effect. In terms of conductivity tensor  $\sigma_{ij}$ , the effect is represented by antisymmetric components  $\sigma_{ij}^F \propto \epsilon_{ijk} M_k$ . This is the form allowed by the Onsager relation at the linear order in  $\mathbf{M}$ , which breaks time-reversal invariance.

In the presence of magnetization structure, spatial derivatives  $\nabla_i M_j$ , which break the symmetries of both time reversal and spatial inversion, have different effects. Such derivatives have the same symmetry as toroidal moment and lead to intriguing phenomena such as nonreciprocal propagation and reflection as studied in Refs.<sup>50–53</sup>.

In this paper, we study the effects of derivatives of the form  $M_i \nabla_j M_k$ . These terms break spatial inversion keeping the time-reversal invariance and are equivalent to spin current and chirality from the symmetry. In fact, the components symmetric with respect to  $i$  and  $k$  are trivial if  $|\mathbf{M}|$  is constant and the medium is isotropic, while the antisymmetric represent equilibrium spin current carried by non-collinear magnetization structures:

$$J_{ij}^S \propto \epsilon_{ikl} M_i \nabla_j M_k. \quad (2)$$

Chiral response called the optical activity, represented by the off-diagonal conductivity tensor  $\sigma_{ij}^C \propto \epsilon_{ijk} q_k$ , where  $\mathbf{q}$  is the wave vector of the electromagnetic wave, arises from  $J_{ij}^S$ , as known in magnetic chiral systems. For isotropic responses independent of  $\mathbf{q}$  to arise from  $J_{ij}^S$ , another interaction breaking inversion symmetry is necessary. Here we consider the case of Rashba spin-orbit interaction defined by the hamiltonian<sup>2,48</sup>

$$\hat{H}_R = i(\boldsymbol{\alpha}_R \cdot [\nabla \times \hat{\boldsymbol{\sigma}}]), \quad (3)$$

with the Rashba vector  $\boldsymbol{\alpha}_R$ . The general form allowed is

$$\sigma_{qp} \propto \gamma_{qplmn} J_{mn}^S \alpha_{Rl}, \quad (4)$$

where  $\gamma_{qplmn}$  is a rank five tensor. It gives rise to a diagonal conductivity for some magnetization distributions, as shown below. We define a charge counting the pitch of magnetization variation in the plane of magnetization by

$$Q_i \propto \epsilon_{ijk} J_{jk}^S \equiv \epsilon_{ijk} [\mathbf{M} \times \nabla_k \mathbf{M}]_j. \quad (5)$$

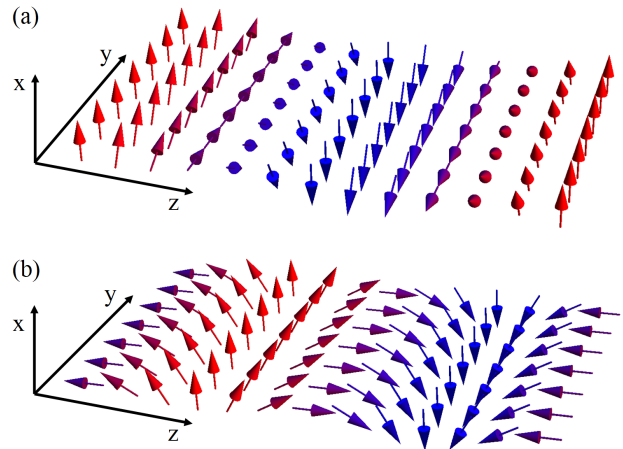


FIG. 1. (Color online) Magnetic helicoid (a) and magnetic cycloid (b).

After summing up two Levi-Civita tensors, this equation has the form  $Q_i \propto (\delta_{ku} \delta_{iv} - \delta_{kv} \delta_{iu}) M_u \nabla_k M_v$  indicating that the electric polarization  $\mathbf{P}_{me}$  of Eq. (1) agrees with  $\mathbf{Q}$ . Taking into account that  $|\mathbf{M}| = \text{const}$  this is written as

$$\mathbf{Q} \propto (\mathbf{M} \text{div} \mathbf{M} + [\mathbf{M} \times \text{rot} \mathbf{M}]) \quad (6)$$

which is also known from literature<sup>28</sup>.

The conductivity is related to electric permittivity  $\epsilon_{ij}$  by  $\hat{\epsilon} = \frac{4\pi i}{\Omega} \hat{\sigma}$  for the correction to both tensors due to non-collinear magnetization where  $\Omega$  is the electromagnetic wave frequency. The above consideration therefore shows electric polarization

$$\mathbf{P} = \frac{1}{4\pi} \hat{\epsilon} \mathbf{E} \quad (7)$$

generated by the Rashba spin-orbit interaction and magnetic spin current when an electric field  $\mathbf{E} \propto \exp(-i\Omega t)$  of the electromagnetic wave is applied. General form of such polarization allowed by symmetry is

$$P_q = \frac{i}{\Omega} \gamma_{qplmn} J_{mn} \alpha_{Rl} E_p, \quad (8)$$

where  $\gamma_{qplmn}$  is the tensor that determines conductivity in (4). It should be noted that this tensor should contain only the Kronecker delta and antisymmetric Levi-Civita tensor if the medium is isotropic.

We consider two typical magnetization structures, helicoid and cycloid (see Figure 1). The magnetization normalized to unit in the Cartesian coordinate system is

$$\mathbf{M} = (\cos qz, \sin qz, 0) \quad (9)$$

for helicoid and

$$\mathbf{M} = (-\cos qz, 0, \sin qz) \quad (10)$$

for cycloid,  $q = 2\pi/L$  is the wavenumber determined by the helicoid (cycloid) period  $L$ , and the Cartesian coordinate system is introduced according to Figure 1. Magnetic distributions (9) and (10), despite being very similar, have different symmetry properties. For the helicoid, there is only  $J_{zz}^S$  while the cycloid has non-zero  $J_{yz}^S$  and thus the vector  $\mathbf{Q} \propto qe_x$  along the  $x$ -axis.

We expect following terms in conductivity for magnetic helicoid and cycloid. We consider first the magnetic helicoid described by (9). For  $\alpha_R||ox$  we have finite  $\sigma_{zy}$  and  $\sigma_{yz}$ , and for  $\alpha_R||oy$  —  $\sigma_{zx}$  and  $\sigma_{xz}$ . For  $\alpha_R||oz$  (along the magnetization change direction)  $\sigma_{xy} = -\sigma_{yx}$  appears. Denoting the dielectric permittivity linear in  $\alpha_R$  and for  $\alpha_R$  along the  $i$ -th Cartesian axis as  $\hat{\varepsilon}^{(i)}$ , we have:

$$\hat{\varepsilon}^{(x)} = \frac{q\alpha_R}{\Omega} \begin{pmatrix} 0 & 0 & 0 \\ 0 & 0 & B_1 + iB_2 \\ 0 & B_1 - iB_2 & 0 \end{pmatrix}, \alpha_R||ox, \quad (11)$$

$$\hat{\varepsilon}^{(y)} = -\frac{q\alpha_R}{\Omega} \begin{pmatrix} 0 & 0 & B_1 + iB_2 \\ 0 & 0 & 0 \\ B_1 - iB_2 & 0 & 0 \end{pmatrix}, \alpha_R||oy, \quad (12)$$

$$\hat{\varepsilon}^{(z)} = \frac{q\alpha_R}{\Omega} \begin{pmatrix} 0 & -iB_3 & 0 \\ iB_3 & 0 & 0 \\ 0 & 0 & 0 \end{pmatrix}, \alpha_R||oz, \quad (13)$$

where  $B_j$  are constants. Although all constants  $B_j$  are generally complex they should obey the Onsager relations<sup>47</sup>; if there is no dissipation in the system, all these constants are real. As one should expect,  $\hat{\varepsilon}^{(x)}$  for  $\alpha_R||ox$  (determined by (11)) and  $\hat{\varepsilon}^{(y)}$  for  $\alpha_R||oy$  (determined by (12)) are identical and differ only by coordinate system transform (namely, rotation by  $90^\circ$  and change of the direction of one of the axes to opposite). This is governed by the fact that we consider infinite medium hence two directions perpendicular to the spiral axis are similar. The dielectric permittivity in these cases contains both antisymmetric term determined by  $B_2$  and symmetric one determined by  $B_1$ . The  $\hat{\varepsilon}^{(z)}$  tensor (13) for the case when the Rashba vector is along the spiral axis  $oz$  is different: only antisymmetric hyrotropic term exists. Note that the dielectric permittivity is described by off-diagonal terms for any direction of  $\alpha_R$ . Therefore only polarization effects such as polarization rotation arise for helicoid and no intensity effects are possible.

For the magnetic cycloid described by (10) three cases are possible. For  $\alpha_R||ox$  there are three diagonal terms  $\sigma_{xx}, \sigma_{yy}, \sigma_{zz}$ . For  $\alpha_R||oy$  we have  $\sigma_{yx}$  and  $\sigma_{xy}$ ; for  $\alpha_R||oz$

—  $\sigma_{zx}$  and  $\sigma_{xz}$ . The dielectric permittivity has the form

$$\hat{\varepsilon}^{(x)} = \frac{q\alpha_R}{\Omega} \begin{pmatrix} C_1 & 0 & 0 \\ 0 & C_2 & 0 \\ 0 & 0 & C_3 \end{pmatrix}, \alpha_R||ox, \quad (14)$$

$$\hat{\varepsilon}^{(y)} = \frac{q\alpha_R}{\Omega} \begin{pmatrix} 0 & C_4 + iC_5 & 0 \\ C_4 - iC_5 & 0 & 0 \\ 0 & 0 & 0 \end{pmatrix}, \alpha_R||oy, \quad (15)$$

$$\hat{\varepsilon}^{(z)} = \frac{q\alpha_R}{\Omega} \begin{pmatrix} 0 & 0 & C_6 + iC_7 \\ 0 & 0 & 0 \\ C_6 - iC_7 & 0 & 0 \end{pmatrix}, \alpha_R||oz \quad (16)$$

where  $C_j$  are constants (which are real in the absence of dissipation followed by the Onsager relations). For three perpendicular directions of  $\alpha_R$ . All three directions are different here. The  $x$ -direction is distinguished by the fact that the Rashba vector is along the direction of the magnetoelectric vector  $\mathbf{Q}$  which leads to correction to the diagonal permittivity (14). This, in turn, should give rise to the intensity effect. In two other cases,  $\alpha_R$  along  $oy$  or along  $oz$ , there are off-diagonal terms, which lead to polarization effects. The constants  $C_{4,5}$  in (15) and  $C_{6,7}$  in (16) that determine the dielectric permittivity for  $\alpha_R$  along  $oy$  and along  $oz$  are independent and cannot be connected to each other. This is clear from the fact that there is no symmetry relation between the  $y$  and  $z$  direction for the considered magnetization distribution.

It is worth noting that in comparison to helicoid, the cycloid seems to be more complicated. First, there are seven independent constants determining the permittivity in different geometric configurations for the cycloid, while only three constants are needed for the helicoid. Second, there are three cases that cannot be connected symmetrically in cycloid and two different cases in helicoid. Third, the cycloid represents a wider range of physical phenomena, including the magnetoelectric polarization and the intensity optical effect that are forbidden in the helicoid. However, in what follows we will see that calculations are more simple for the cycloid due to some hidden symmetry which allows to find the exact answer, while it is not possible for the helicoid.

As for the intensity of optical response, it is governed by a scalar, which in the present case of the Rashba interaction and spin current is  $\epsilon_{ijk}\alpha_R i J_{jk}^S = (\alpha \cdot \mathbf{Q})$  (averaged over polarizations of light). It is clear that there is no intensity effect for the helicoid, but it exists for the cycloid if the Rashba vector  $\alpha_R$  is parallel to the  $x$ -axis (see Figure 1). This is obvious from our previous analysis of electric conductivity: the diagonal terms exist only for the magnetic cycloid with  $\alpha_R||ox$ , and this leads to the intensity effect which does not vanish after averaging over polarizations of light.

### III. MICROSCOPIC CALCULATIONS

Our microscopic calculations are based on the non-equilibrium Green's functions formalism<sup>49</sup>. We start

with the hamiltonian

$$\hat{H} = \hat{H}_0 + \hat{H}_{sd} + \hat{H}_R, \quad (17)$$

where  $\hat{H}_R$  is the Rashba hamiltonian determined by (3),  $\hat{H}_0$  is the free electron hamiltonian that takes form in the presence of the external field determined by a vector-potential  $\mathbf{A}^{\text{em}}$ :

$$\hat{H}_0 = -\frac{\hbar^2}{2m} \left( \nabla - i\frac{e}{\hbar} \mathbf{A}^{\text{em}} \right)^2, \quad (18)$$

$\hbar$  here is the Planck constant,  $m$  and  $e$  are the electron mass and charge.  $\hat{H}_{sd}$  in (17) is the s-d exchange interaction hamiltonian that has the form

$$\hat{H}_{sd} = -J(\mathbf{M} \cdot \boldsymbol{\sigma}), \quad (19)$$

$\boldsymbol{\sigma}$  is the Pauli matrix vector, and we introduce the exchange constant  $J$ , thus supposing that the magnetization  $\mathbf{M}$  is normalized to unit:  $|\mathbf{M}| = 1$ . We suppose that the direction of magnetization depends on coordinates while its absolute value remains constant, thus  $J$  does not depend on coordinates. It is important to note that we suppose the Rashba coupling to be relatively weak and therefore are interested in lowest-order (linear) corrections with respect to it. The magnetization is also supposed to change in space slowly (typical magnetization change length is smaller than the electron oscillations scale in the wave electric field) and therefore we restrict ourselves with the first-order derivatives of  $\mathbf{M}$ . Besides, integration over space is implicitly supposed in the field hamiltonians below.

In terms of second quantization the hamiltonian may be re-written as<sup>2</sup>

$$\begin{aligned} \hat{H} = & \frac{\hbar^2}{2m} \hat{c}^\dagger \overleftarrow{\nabla} \overrightarrow{\nabla} \hat{c} + i\frac{e\hbar}{2m} \mathbf{A}_m^{\text{em}} \hat{c}^\dagger \overleftarrow{\nabla} \hat{c} + \quad (20) \\ & \frac{e^2}{2m} (A^{\text{em}})^2 \hat{n} - J(\mathbf{M} \cdot \hat{c}^\dagger \boldsymbol{\sigma} \hat{c}) + \\ & \frac{i}{2} \hat{c}^\dagger \left( \boldsymbol{\alpha}_R \cdot \left[ \overleftarrow{\nabla} \times \boldsymbol{\sigma} \right] \right) \hat{c}, \end{aligned}$$

where we use Greek symbols to denote the spin coordinates, i.e.

$$A_i^{S,R} = \sigma_\alpha A_i^{S,R\alpha}, \quad (27)$$

and the gradient part of the current operator and the

where  $\hat{c}^+$  and  $\hat{c}$  are the operators of electron nucleation and destruction,  $\hat{n} \equiv \hat{c}^+ \hat{c}$  is the density operator,  $\overleftarrow{\nabla}$  and  $\overrightarrow{\nabla}$  act on the expressions to the right and to the left respectively,  $\overleftrightarrow{\nabla} \equiv \overrightarrow{\nabla} - \overleftarrow{\nabla}$ . We rotate local spin coordinate system so that the  $z$  axis of a new coordinate system is parallel to magnetization. The unitary operator of spin coordinate transform has the form

$$U = m_i \sigma_i, \quad (21)$$

where the vector  $\mathbf{m}$  is determined by the spherical coordinates of  $\mathbf{M}$ ,  $\phi$  and  $\theta$ , as<sup>2</sup>

$$\mathbf{m} = \left( \cos \phi \sin \frac{\theta}{2}, \sin \phi \sin \frac{\theta}{2}, \cos \frac{\theta}{2} \right) \quad (22)$$

which depends on the coordinate:  $U = U(\mathbf{r})$ . The new operators of electron nucleation and destruction are defined simply as  $\hat{a} = U\hat{c}$ ,  $\hat{a}^+ = \hat{c}^+U$ . The hamiltonian in new coordinate system may be written as:

$$\begin{aligned} \hat{H} = & \frac{\hbar^2}{2m} \hat{a}^\dagger \overleftarrow{\nabla} \overrightarrow{\nabla} \hat{a} - J\hat{a}^\dagger \sigma_z \hat{a} - \quad (23) \\ & \hat{a}^\dagger \left( -i\frac{e\hbar}{2m} \overleftarrow{\nabla} - \frac{e^2}{m} \mathbf{A}_\Sigma \right) \mathbf{A}_\Sigma \hat{a} - \frac{e^2}{2m} \hat{a}^\dagger \mathbf{A}_\Sigma^2 \hat{a}, \end{aligned}$$

where  $\overleftarrow{\nabla}$  acts only on operators  $\hat{a}^+$  and  $\hat{a}$ . Here we introduce the effective vector-potential

$$\mathbf{A}_\Sigma = \mathbf{A}^{\text{em}} + \mathbf{A}^S + \mathbf{A}^R, \quad (24)$$

$\mathbf{A}^S$  and  $\mathbf{A}^R$  are the additional vector-potentials that appear due to spin texture and due to Rashba coupling correspondingly. These vector-potentials are determined as:

$$\mathbf{A}^S = i\frac{\hbar}{e} U^\dagger \nabla U, \quad \mathbf{A}^R = -\frac{m}{e\hbar} [\boldsymbol{\alpha}_R \times U^\dagger \boldsymbol{\sigma} U]. \quad (25)$$

Note that, comparing to Ref.<sup>2</sup>, we have no time dependence of  $U$ . Therefore there is no need to write the Lagrangian, and no additional vector-potential due to  $\partial_t U$  appears.

The hamiltonian (23) may be re-written in a more useful form:

$$\begin{aligned} \hat{H} = & \frac{\hbar^2}{2m} \hat{a}^\dagger \overleftarrow{\nabla} \overrightarrow{\nabla} \hat{a} - J\hat{a}^\dagger \sigma_z \hat{a} - \hat{a}^\dagger \mathbf{j}_\nabla \cdot \mathbf{A}^{\text{em}} \hat{a} - \hat{a}^\dagger e J_i^\alpha A_i^{S\alpha} \hat{a} - \hat{a}^\dagger e J_i^\alpha A_i^{R\alpha} \hat{a} + \quad (26) \\ & \hat{a}^\dagger \frac{e^2}{2m} \left( (A^{\text{em}})^2 + (A^S)^2 \right) \hat{a} + \frac{e^2}{m} \hat{a}^\dagger \mathbf{A}^{\text{em}} \cdot \mathbf{A}^S \hat{a} + \frac{e^2}{m} \hat{a}^\dagger \mathbf{A}^{\text{em}} \cdot \mathbf{A}^R \hat{a} + \frac{e^2}{m} \hat{a}^\dagger A_i^{S\alpha} A_i^{R\alpha} \hat{a}, \end{aligned}$$

spin current operator are

$$\mathbf{j}_\nabla = -i\frac{e\hbar}{2m} \overleftarrow{\nabla}, \quad J_i^\alpha = -i\frac{\hbar}{2m} \overleftarrow{\nabla}_i \sigma_\alpha. \quad (28)$$

The hamiltonian (26) contains separate parts linear in

$\mathbf{A}^{\text{em}}, \mathbf{A}^S, \mathbf{A}^R$  (third, fourth and fifth terms in the right side), cross-terms that are linear in two different  $\mathbf{A}$ 's (seventh, eighth and ninth terms in the right side) and terms that are quadratic in  $\mathbf{A}^{\text{em}}, \mathbf{A}^S$  (sixth term in the right side). Note that there is no term quadratic in  $\mathbf{A}^R$  which is caused by the spin part of  $(\mathbf{A}^R)^2$ . We are interested in linear response to  $\mathbf{A}^{\text{em}}$  and also in lowest-order linear terms in  $\mathbf{A}^S, \mathbf{A}^R$  and therefore there is no need to take these quadratic terms into account. However the cross-terms are important.

It follows from (23) and (26) that the operator of current has the form

$$\mathbf{j} = \mathbf{j}_\nabla - \frac{e^2}{m} (\mathbf{A}^{\text{em}} + \mathbf{A}^S + \mathbf{A}^R). \quad (29)$$

In order to find the linear optical response in the absence of spatial dispersion, we take

$$\mathbf{A}^{\text{em}} = \frac{1}{i\Omega} \mathbf{E}, \quad (30)$$

$\Omega$  is the electromagnetic wave frequency, and calculate the electric current induced by it. The electric polarization  $\mathbf{P}$  may be found if the induced average electric current is known:

$$\mathbf{P} = \frac{i}{\Omega} \mathbf{j}. \quad (31)$$

Thus the main goal is to find the electric current induced by the wave. The non-equilibrium Green's function method that we use is described elsewhere<sup>2,49</sup>. The non-perturbed Green function takes into account the magnetization along the  $z$ -axis and is described after Fourier transform by the formula:

$$\hat{g}^r[\mathbf{k}, \omega] = \frac{1}{\hbar\omega - \epsilon_\pm(\mathbf{k}) + i\hbar\eta}, \quad (32)$$

$$\hat{g}^a[\mathbf{k}, \omega] = \frac{1}{\hbar\omega - \epsilon_\pm(\mathbf{k}) - i\hbar\eta}, \quad (33)$$

$$\hat{g}^<[\mathbf{k}, \omega] = 2\pi i f(\omega) \delta(\hbar\omega - \epsilon_\pm(\mathbf{k})), \quad (34)$$

where  $\hat{g}^r, \hat{g}^a, \hat{g}^<$  are the retarded, advanced and lesser Green functions correspondingly,  $\eta = \frac{1}{2\tau_e}$  is the frequency of electron scattering on impurities,  $\epsilon_\pm(\mathbf{k})$  is the energy of electron:

$$\epsilon_\pm(\mathbf{k}) = \frac{\hbar^2 k^2}{2m} \mp J, \quad (35)$$

$f$  is the electron distribution function:

$$f(\omega) = \frac{1}{\exp\left(\frac{\hbar\omega - \epsilon_F}{k_B T}\right) + 1} \approx \text{st}(\epsilon_F - \hbar\omega). \quad (36)$$

Here we suppose that temperature  $T$  is zero;  $\epsilon_F$  is the Fermi energy,  $\text{st}()$  is the Heaviside theta function. Obviously, the Green functions are spin-dependent and therefore have implied indices. After substituting  $\omega$  from the

delta-function in (34) the distribution function also becomes spin-dependent:

$$f_\pm(k) = \text{st}(\epsilon_F - \epsilon_\pm(\mathbf{k})). \quad (37)$$

The linear in  $\mathbf{E}$  current is determined by equation

$$\tilde{\mathbf{j}}(\mathbf{r}, t) = -i\hbar \text{tr} [j G^<(\mathbf{r}, t, \mathbf{r}, t)], \quad (38)$$

where  $G^<$  is the lesser Green function calculated in the first order in  $\mathbf{A}^{\text{em}}, \mathbf{A}^S, \mathbf{A}^R$ . We calculate its Fourier transform and then perform the inverse transform. The current, linear in  $\mathbf{A}^S$  and  $\mathbf{A}^R$ , follows from equations (26) and (29). It may be represented in the form of diagrams shown in Figure 2. Including all permutations, there are 21 diagrams totally. Considering particular distributions of magnetization which are periodic in space we average the current over this period:  $\langle \mathbf{j} \rangle = \frac{1}{V} \int_V \tilde{\mathbf{j}} d^3\mathbf{r}$

The reason for the induced polarization to appear due to spin texture and Rashba coupling is the transition between spin subbands that is allowed due to the interplay of spin texture and spin-orbit interaction. Indeed, both  $\mathbf{A}^S$  and  $\mathbf{A}^R$  in Figure 2 change the electron spin. This leads to a non-zero result after averaging. The resulting average current in general case is very complicated. Its full form is written in the Appendix. In the following section we analyse some properties of this result for the magnetic helicoid (9) and magnetic cycloid (10).

## IV. RESULTS AND DISCUSSION

### A. Helical magnetization distribution

The induced electric current is found for helical magnetic moment distribution (9) by substituting into general result (see the Appendix) following vector-potentials (in the momentum space):

$$\mathbf{A}^S[\mathbf{p}] = \frac{\hbar q}{2e} (2\pi)^3 \delta(p_x) \delta(p_y) \mathbf{e}_z (-\delta(p_z) \sigma_z + \delta(p_z - q) \frac{\sigma_x - i\sigma_y}{2} + \delta(p_z + q) \frac{\sigma_x + i\sigma_y}{2}), \quad (39)$$

$$\mathbf{A}_{(z)}^R = -\frac{m\alpha_R}{2e\hbar} (2\pi)^3 \delta(p_x) \delta(p_y) \times (\mathbf{e}_x (\delta(p_z) \sigma_y + i(\delta(p_z - q) - \delta(p_z + q)) \sigma_z) + \mathbf{e}_y (-\delta(p_z) \sigma_x + (\delta(p_z - q) + \delta(p_z + q)) \sigma_z)), \quad (40)$$

$$\mathbf{A}_{(x)}^R = -\frac{m\alpha_R}{2e\hbar} (2\pi)^3 \delta(p_x) \delta(p_y) \times (\mathbf{e}_y (-\delta(p_z - q) (\sigma_x - i\sigma_y) - \delta(p_z + q) (\sigma_x + i\sigma_y)) + \mathbf{e}_z (i\sigma_z (\delta(p_z + q) - \delta(p_z - q)) - \delta(p_z) \sigma_y)), \quad (41)$$

where  $\mathbf{A}_{(z)}^R$  and  $\mathbf{A}_{(x)}^R$  correspond to  $\alpha_R$  parallel to  $z$  and  $x$ , and we neglect the  $p_z$  shifted by  $2q$  in  $\mathbf{A}^R$  since it does not contribute to final result for current. It is important to note that we choose the coordinate system such that

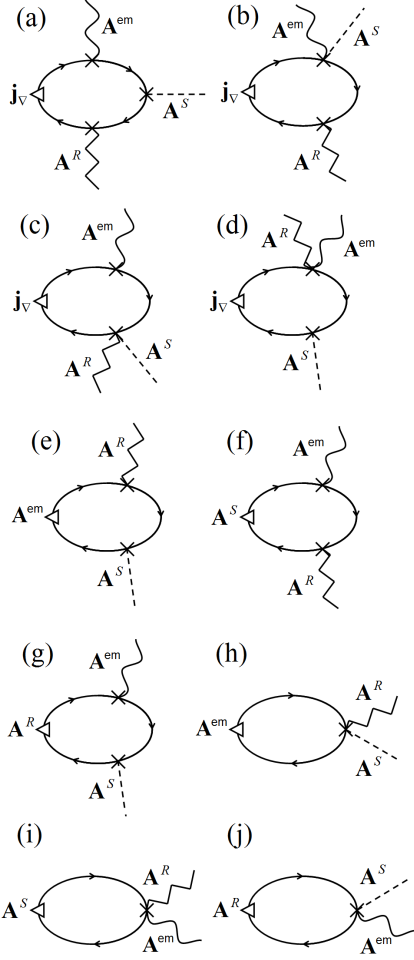


FIG. 2. Diagrammatic representation of the linear electric current induced by electromagnetic wave in the presence of spin texture and Rashba coupling. The permutations are omitted. The  $\mathbf{A}^{\text{em}}$ ,  $\mathbf{A}^S$ ,  $\mathbf{A}^R$  symbols correspond to the terms linear in these vector potentials (either in hamiltonian or in current operator).

the helicoid axis is along the Cartesian  $z$ -coordinate, and the Rashba vector is either along the  $z$ - or along the  $x$ -coordinate (parallel or perpendicular to the helicoid axis). Since we take into account only the terms linear in the Rashba interaction this represents the general case.

For  $\alpha_R \parallel oz$ , substituting  $\mathbf{A}^S$  and  $\mathbf{A}^R$  into the current gives zero. This is governed by additional symmetry of the helical magnetization distribution<sup>54</sup> that leads to zero  $B_3$  coefficient in (13). For the Rashba vector along  $x$ -axis there is non-zero response. It corresponds to  $\sigma_{zy}$  and  $\sigma_{yz}$  which are nonzero in this case. This is expected from symmetry equation (11) in which  $\varepsilon_{yz}^{(x)}$  and  $\varepsilon_{zy}^{(x)}$  are determined by two independent coefficients  $B_1$  and  $B_2$ . These coefficients are not real in our calculations since dissipation is taken into account by introducing  $\eta$ .

## B. Cycloidal magnetization distribution

We will consider the cycloidal magnetic moment distribution in detail since it is possible to obtain a simple and interesting result for this distribution. Using (10) and (25) one may obtain following vector-potentials (in the momentum space):

$$\mathbf{A}^S[\mathbf{p}] = -\frac{\hbar q}{2e} (2\pi)^3 \delta(p_x) \delta(p_y) \delta(p_z) \mathbf{e}_z \sigma_y, \quad (42)$$

$$\mathbf{A}_{(x)}^R = \frac{m\alpha_R}{e\hbar} (2\pi)^3 \delta(p_x) \delta(p_y) (\mathbf{e}_z \sigma_y \delta(p_z) - \mathbf{e}_y \left( \delta(p_z - q) \frac{\sigma_x + i\sigma_z}{2} + \delta(p_z + q) \frac{\sigma_x - i\sigma_z}{2} \right)), \quad (43)$$

$$\mathbf{A}_{(y)}^R = \frac{m\alpha_R}{e\hbar} (2\pi)^3 \delta(p_x) \delta(p_y) \times \left( \mathbf{e}_x \left( \delta(p_z - q) \frac{\sigma_z - i\sigma_x}{2} + \delta(p_z + q) \frac{\sigma_z + i\sigma_x}{2} \right) - \mathbf{e}_z \left( \delta(p_z - q) \frac{\sigma_x + i\sigma_z}{2} + \delta(p_z + q) \frac{\sigma_x - i\sigma_z}{2} \right) \right), \quad (44)$$

$$\mathbf{A}_{(z)}^R = \frac{m\alpha_R}{e\hbar} (2\pi)^3 \delta(p_x) \delta(p_y) (-\mathbf{e}_x \sigma_y \delta(p_z) + \mathbf{e}_y \left( \delta(p_z - q) \frac{\sigma_z - i\sigma_x}{2} + \delta(p_z + q) \frac{\sigma_z + i\sigma_x}{2} \right)) \quad (45)$$

where  $\mathbf{A}_{(i)}^R$  denotes the vector-potential in the case when  $\alpha_R \parallel oi$ . It follows from (42) and (44) that the induced electric current for  $\alpha_R$  along the  $y$ -axis is zero. This is obvious from the momentum conservation:  $\mathbf{A}^S$  does not change momentum in this case, while  $\mathbf{A}^R$  changes.

The magnetic cycloid has high symmetry ( $\mathbf{A}^S$  is constant in the real space) which leads to a possibility to integrate everything exactly here. The electric current that appears as a response to the electromagnetic wave electric field is calculated by substituting (42)-(45) to the equations provided in the Appendix and taking integrals (note that two delta-functions provided by  $\mathbf{A}^S$  and  $\mathbf{A}^R$  should have the same argument; accurately taking into account this distribution leads to vanishing of one of the integrals and the term  $\frac{(2\pi)^3}{V}$ , while the second integral may be taken exactly). Using (31) and (7) it is convenient to get the result for optical response in terms of the dielectric permittivity  $\hat{\varepsilon}$ . For  $\alpha_R$  along  $x$ - and  $z$ -directions, we have

$$\hat{\varepsilon}^{(x)} = 4\pi \frac{e^2 \hbar^2}{m} N_e q \alpha_R \epsilon_F \times \begin{pmatrix} \frac{2}{5}F_1 + \frac{2}{7}F_2 & 0 & 0 \\ 0 & \frac{2}{5}F_1 + \frac{2}{35}F_2 & 0 \\ 0 & 0 & \frac{2}{5}F_1 + \frac{2}{35}F_2 \end{pmatrix}, \quad (46)$$

$$\hat{\varepsilon}^{(z)} = 4\pi \frac{e^2 \hbar^2}{m} N_e q \alpha_R \epsilon_F \times \begin{pmatrix} 0 & 0 & -\frac{2}{35}F_2 \\ 0 & 0 & 0 \\ -\frac{2}{35}F_2 & 0 & 0 \end{pmatrix} \quad (47)$$

respectively, where  $N_e = \frac{1}{3\pi^2} \left( \frac{2m}{\hbar^2} \epsilon_F \right)^{3/2}$  is the electron density, and the frequency dependent functions  $F_{1,2}(\hbar\Omega)$  are determined as

$$F_1 = \frac{1}{(\hbar\Omega)^2} \left( \frac{3}{4J^2 + (\hbar\eta)^2} - \frac{1}{(\hbar\Omega + i\hbar\eta)^2} \right), \quad (48)$$

$$F_2 = \frac{1}{(\hbar\Omega)^2} \frac{4J^2}{4J^2 - (\hbar\Omega + i\hbar\eta)^2} \times \left( \frac{1}{(\hbar\eta)^2} + \frac{1}{(\hbar\Omega + i\hbar\eta)^2} - \frac{2}{4J^2 + (\hbar\eta)^2} \right). \quad (49)$$

It is important that the obtained dielectric permittivity tensors obey the Onsager relations<sup>47</sup>; however one should take into account that  $\eta$  has dissipative roots and therefore changes sign under time reversal. The result obtained in (46)–(49) corresponds to the symmetry consideration (14)–(16); note that constant  $C_7$  is zero for  $\alpha_R||oz$ . The zero result for  $\alpha_R||oy$  is not predicted by symmetry considerations ( $C_4$  and  $C_5$  in (15) are zero from calculations). It follows from additional hidden symmetry of the system: the vector-potential provided by spin texture is constant.

Equations (46)–(49) allow to estimate the value of the effect and to investigate its frequency dependence. It is interesting to analyze the case of  $\alpha_R||ox$  because in this case the intensity effect occurs. For estimation, we take  $\epsilon_F = 5$  eV,  $N_e = 5 \cdot 10^{22}$  cm<sup>-3</sup>,  $\hbar\eta = 0.1$  eV which are typical for metals. The exchange energy  $J = 1$  eV, and  $L \equiv \frac{2\pi}{q} = 20$  nm. The Rashba constant is quite well known for semiconductors and is of the order of value  $\alpha_R \approx 1$  peV · m which we take for estimations. Real and imaginary parts of the addition to the dielectric permittivity  $\hat{\epsilon}^{(x)}$  for these parameters with respect to frequency is plotted in Figure 3. It is seen that the addition to  $\hat{\epsilon}$  is rather big. For instance, the correction to dielectric permittivity for red light ( $\hbar\Omega = 0.31$  eV) is estimated as  $\hat{\epsilon}_{xx}^{(x)} = 32.16 + 1.23i$  for the chosen parameters which would be large enough for experimental observations of the investigated effect.

An important property seen from Figure 3 is the resonance due to the exchange splitting. It follows from electron transitions between spin subbands which is allowed in the presence of spin texture<sup>55</sup> or spin-orbit interaction. The resonant frequency is

$$\hbar\Omega_r = \sqrt{4J^2 + \hbar^2\eta^2} \quad (50)$$

which corresponds to  $\hbar\Omega_r \approx 2$  eV in Figure 3. The imaginary part of the correction to the dielectric permittivity has a maximum at resonant frequency. This corresponds to strong absorption of the electromagnetic wave. Similar absorption was predicted earlier<sup>55</sup>, but only spin texture was taken into account and thus it appeared solely due to the exchange interaction. Here we have another addition that is caused by Rashba coupling together with the spin texture.

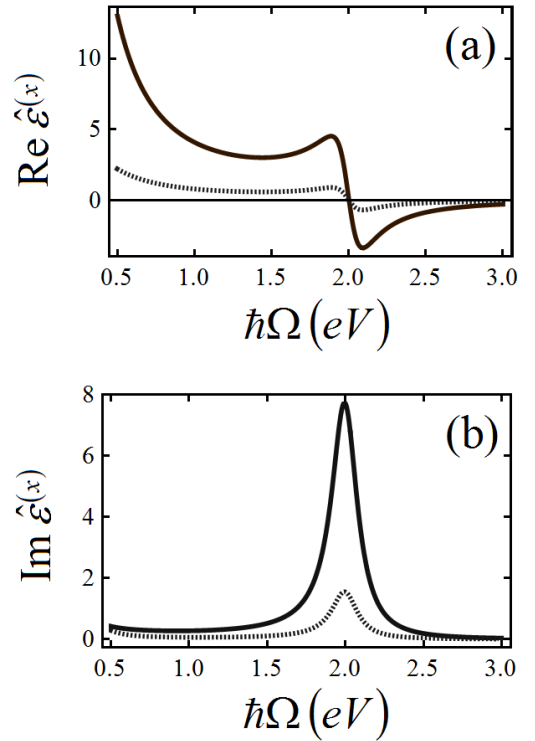


FIG. 3. Dependence of real (a) and imaginary (b) part of dimensionless  $\hat{\epsilon}^{(x)}$  on wave frequency. Solid line is  $\epsilon_{xx}^{(x)}$ , dotted line is  $\epsilon_{yy}^{(x)}, \epsilon_{zz}^{(x)}$ .

The real part of correction to the dielectric permittivity changes sign at the resonance frequency. It has a maximum of absolute value and tends to zero as the frequency tends to infinity. The frequency at which the maximum of absolute value occurs can be roughly estimated as

$$\hbar\Omega_m \approx \hbar\Omega_r + \hbar\eta \quad (51)$$

if  $\hbar\eta \ll J$  is assumed. The resonance becomes bigger and sharper as  $\hbar\eta \rightarrow 0$  both for absorption and real part of permittivity. Also it should be noted that we perform the calculations supposing that the frequency of electron scattering on impurities is small (see (34):

$$\eta \ll \Omega. \quad (52)$$

Therefore the result obtained in (46)–(49) is valid only for  $\Omega$  satisfying the condition (52).

An important effect investigated here is the addition to the intensity of light in a system with Rashba coupling (with a surface) that has the flexo-magnetoelectric vector  $\mathbf{Q}$ . The magnetization distribution that allows for the existence of this vector may appear at the boundary of a ferromagnet and a heavy metal due to the Dzyaloshinskii-Moriya interaction (DMI)<sup>56–59</sup>. Such distribution was previously observed at a boundary of Ir(111) and Fe<sup>60</sup>. In these quite sophisticated experiments the measurements

were performed by spin-resolved scanning tunneling microscopy. One, two and three monolayers of Fe were used, and the fabrication and all measurements were performed in a vacuum chamber. The properties of the observed magnetic cycloid strongly depended on the number of monolayers. Only the three-monolayer structure showed the cycloid at room temperature with the spatial scale  $L = 65nm$ . This scale became much smaller as the temperature decreased. Parts of surface with four monolayers did not have the observable magnetic cycloid distribution. However if a thicker magnetic layer is taken it should slightly oscillate about the uniform magnetization close to the surface with DMI. These oscillations would give rise to the intensity magneto-optical effect in the reflected light. Such intensity effect should be measured in meridional geometry. Applying an external magnetic field would change the magnetization distribution to uniform and destroy the effect. This effect should be small because the magnitude of magnetization oscillations due to DMI should be small. On the other hand, the effect grows as the magnetization scale  $L$  is made smaller, and it was shown experimentally that  $L$  becomes smaller at small temperature. Thus, the optical effect considered in this paper could be observed in proper conditions.

Another possible opportunity is to observe the new intensity effect in multiferroics such as bismuth ferrite  $\text{BiFeO}_3$  where the magnetic cycloid exists at room temperature<sup>28,61-63</sup> and the existence of electric polarization is known.

## V. CONCLUSION

In summary, we have theoretically investigated the new linear magneto-optical effect that appears in non-collinear magnetic systems with Rashba spin-orbit interaction. This effect is caused by electron movement in non-uniform magnetization due to the wave electric field

and may be described by the non-zero tensor of spin current. Obviously, it exists in a system with zero average magnetization. We provide the symmetry analysis and microscopic calculations that correspond to each other. According to our theory, systems with zero diagonal spin current such as a magnetic helicoid demonstrate polarization rotation, i.e. an additional polarization due to new effect is perpendicular to the polarization of incident light. In contrast, systems that have off-diagonal spin current, and particularly the flexo-magneto-electric vector, such as a magnetic cycloid, possess the change of diagonal dielectric permittivity which leads to the intensity effects. If the surface Rashba interaction is directed correctly, the intensity effect may be used to detect the flexo-magneto-electric vector  $\mathbf{Q}$  (which is connected to the Dzyaloshinskii-Moriya interaction<sup>64</sup>) by the optical methods.

## ACKNOWLEDGMENTS

We would like to thank A. Fraerman for valuable discussions. This work was supported by Russian Science Foundation (Grant No. 16-12-10340).

### Appendix: The electric current induced by electromagnetic wave in the presence of spin texture and Rashba current

The electric current is formed by several contributions depicted in Figure 2. Here we provide the results of its calculation for these contributions,  $\tilde{\mathbf{j}}^{(a-j)}$ , averaged over space (the overall current  $\langle \mathbf{j} \rangle = \sum_{\zeta=a..j} \langle \mathbf{j}^{(\zeta)} \rangle$ ). In order to simplify the result, we add a notation  $K$  represented below by (A.1). The resulting current is then written with the usage of this notation in (A.2)-(A.7). Different kinds of brackets  $()$ ,  $[\ ]$ ,  $\{ \}$  are used for the convenience of reading, and  $\langle \rangle$  in the left side stands for the averaging over spatial coordinates.

$$K_{i,j}^{\alpha,\beta}[\mathbf{p}] = \frac{e^{-i\Omega t}}{V} \left( \frac{e^2}{m} \right)^2 \left( A_i^{S\alpha}[-\mathbf{p}] A_j^{R\beta}[\mathbf{p}] + A_j^{S\beta}[\mathbf{p}] A_i^{R\alpha}[-\mathbf{p}] \right), \quad (\text{A.1})$$



$$\begin{aligned}
\langle \mathbf{j}^{(a)} \rangle = & - \sum_{\pm} \int \frac{d\mathbf{p} d\mathbf{k}}{(2\pi)^6} K_{i,j}^{\alpha,\beta}[\mathbf{p}] f_{\pm}(\mathbf{k}) 2A_l^{em} \left( \frac{\hbar^2}{m} \right)^2 \frac{(\mathbf{k} - \frac{\mathbf{p}}{2})_i (\mathbf{k} - \frac{\mathbf{p}}{2})_j}{\hbar\Omega + i\hbar\eta} \left\{ \delta_{\alpha z} \delta_{\beta z} \frac{\frac{\hbar^2}{m} (\mathbf{k}\mathbf{p} - \frac{p^2}{2})}{\frac{\hbar^4}{m^2} (\mathbf{k}\mathbf{p} - \frac{p^2}{2})^2 - (\hbar\Omega + i\hbar\eta)^2} \times (A.2) \right. \\
& \left( k_l \left( \frac{\hbar\Omega (\mathbf{k} - \mathbf{p})}{\frac{\hbar^4}{m^2} (\mathbf{k}\mathbf{p} - \frac{p^2}{2})^2 - (\hbar\eta)^2} + \frac{\mathbf{k}}{\hbar\Omega + i\hbar\eta} \right) - \frac{(\hbar\Omega\mathbf{p} + i\hbar\eta (\mathbf{k} + \mathbf{p})) (k_l - p_l)}{\frac{\hbar^4}{m^2} (\mathbf{k}\mathbf{p} - \frac{p^2}{2})^2 - (\hbar\eta)^2} \right) + ((\delta_{\alpha x} \delta_{\beta x} + \delta_{\alpha y} \delta_{\beta y}) \pm \\
& i (\delta_{\alpha x} \delta_{\beta y} - \delta_{\alpha y} \delta_{\beta x})) \frac{\left( \frac{\hbar^2}{m} (\mathbf{k}\mathbf{p} - \frac{p^2}{2}) \mp 2J \right) \mathbf{k}}{\left( \frac{\hbar^2}{m} (\mathbf{k}\mathbf{p} - \frac{p^2}{2}) \mp 2J \right)^2 - (\hbar\Omega + i\hbar\eta)^2} \left( \frac{-(\hbar\Omega + 2i\hbar\eta) (k_l - p_l)}{\left( \frac{\hbar^2}{m} (\mathbf{k}\mathbf{p} - \frac{p^2}{2}) \mp 2J \right)^2 + (\hbar\eta)^2} + \frac{k_l}{\hbar\Omega + i\hbar\eta} \right) + \\
& ((\delta_{\alpha x} \delta_{\beta x} + \delta_{\alpha y} \delta_{\beta y}) \mp i (\delta_{\alpha x} \delta_{\beta y} - \delta_{\alpha y} \delta_{\beta x})) \left( \frac{(\hbar\Omega + i\hbar\eta) \left( \frac{\hbar^2}{m} (\mathbf{k}\mathbf{p} - \frac{p^2}{2}) \mp 2J \right) (k_l - p_l)}{\left( \left( \frac{\hbar^2}{m} (\mathbf{k}\mathbf{p} - \frac{p^2}{2}) \right)^2 + (\hbar\eta)^2 \right) \left( \left( \frac{\hbar^2}{m} (\mathbf{k}\mathbf{p} - \frac{p^2}{2}) \mp 2J \right)^2 - (\hbar\Omega + i\hbar\eta)^2 \right)} + \right. \\
& \left. \frac{\hbar\Omega k_l \left( \frac{\hbar^2}{m} (\mathbf{k}\mathbf{p} - \frac{p^2}{2}) \pm 2J \right)}{\left( \left( \frac{\hbar^2}{m} (\mathbf{k}\mathbf{p} - \frac{p^2}{2}) \pm 2J \right)^2 + (\hbar\eta)^2 \right) \left( \left( \frac{\hbar^2}{m} (\mathbf{k}\mathbf{p} - \frac{p^2}{2}) \pm 2J \right)^2 - (\hbar\Omega + i\hbar\eta)^2 \right)} \right) (\mathbf{k} - \mathbf{p}) \left. \right\},
\end{aligned}$$

$$\begin{aligned}
\langle \mathbf{j}^{(b,c,d)} \rangle = & \sum_{\pm} \int \frac{d\mathbf{p} d\mathbf{k}}{(2\pi)^6} f_{\pm}(\mathbf{k}) \left\{ -\frac{e^{-i\Omega t}}{V} \left( \frac{e^2}{m} \right)^2 A_i^{S\alpha}[\mathbf{p}] A_i^{R\alpha}[-\mathbf{p}] \frac{2}{(\hbar\Omega + i\hbar\eta)^2} \frac{\hbar^2}{m} (\mathbf{A}^{em} \cdot \mathbf{k}) \mathbf{k} + K_{i,j}^{\alpha,\beta}[\mathbf{p}] + (A.3) \right. \\
& 2A_j^{em} \frac{\hbar^2}{m} \frac{k_i - \frac{p_i}{2}}{\hbar\Omega + i\hbar\eta} \left( \delta_{\alpha z} \delta_{\beta z} \frac{\left( \frac{\hbar^2}{m} (\mathbf{k}\mathbf{p} - \frac{p^2}{2}) \right)^2 - i\hbar\eta (\hbar\Omega + i\hbar\eta) (\hbar\Omega\mathbf{p} + i\hbar\eta (\mathbf{k} + \mathbf{p}))}{\left( \left( \frac{\hbar^2}{m} (\mathbf{k}\mathbf{p} - \frac{p^2}{2}) \right)^2 + (\hbar\eta)^2 \right) \left( \left( \frac{\hbar^2}{m} (\mathbf{k}\mathbf{p} - \frac{p^2}{2}) \right)^2 - (\hbar\Omega + i\hbar\eta)^2 \right)} + ((\hbar\Omega + 2i\hbar\eta) \times \right. \\
& ((\delta_{\alpha x} \delta_{\beta x} + \delta_{\alpha y} \delta_{\beta y}) \pm i (\delta_{\alpha x} \delta_{\beta y} - \delta_{\alpha y} \delta_{\beta x})) \mathbf{k} + (\hbar\Omega + i\hbar\eta) ((\delta_{\alpha x} \delta_{\beta x} + \delta_{\alpha y} \delta_{\beta y}) \mp i (\delta_{\alpha x} \delta_{\beta y} - \delta_{\alpha y} \delta_{\beta x})) (\mathbf{p} - \mathbf{k}) \times \\
& \left. \left. \frac{\left( \frac{\hbar^2}{m} (\mathbf{k}\mathbf{p} - \frac{p^2}{2}) \mp 2J \right)^2 - i\hbar\eta (\hbar\Omega + i\hbar\eta)}{\left( \left( \frac{\hbar^2}{m} (\mathbf{k}\mathbf{p} - \frac{p^2}{2}) \mp 2J \right)^2 + (\hbar\eta)^2 \right) \left( \left( \frac{\hbar^2}{m} (\mathbf{k}\mathbf{p} - \frac{p^2}{2}) \mp 2J \right)^2 - (\hbar\Omega + i\hbar\eta)^2 \right)} \right) \right\},
\end{aligned}$$

$$\begin{aligned}
\langle \mathbf{j}^{(e)} \rangle = & \sum_{\pm} \int \frac{d\mathbf{p} d\mathbf{k}}{(2\pi)^6} K_{i,j}^{\alpha,\beta}[\mathbf{p}] f_{\pm}(\mathbf{k}) \mathbf{A}^{em} \frac{\hbar^2}{m} \left( k_i - \frac{p_i}{2} \right) \left( k_j - \frac{p_j}{2} \right) \left( \frac{\delta_{\alpha z} \delta_{\beta z}}{\left( \frac{\hbar^2}{m} (\mathbf{k}\mathbf{p} - \frac{p^2}{2}) \right)^2 + (\hbar\eta)^2} + (A.4) \right. \\
& \left. \frac{3((\delta_{\alpha x} \delta_{\beta x} + \delta_{\alpha y} \delta_{\beta y}) \pm i (\delta_{\alpha x} \delta_{\beta y} - \delta_{\alpha y} \delta_{\beta x}))}{\left( \frac{\hbar^2}{m} (\mathbf{k}\mathbf{p} - \frac{p^2}{2}) \mp 2J \right)^2 + (\hbar\eta)^2} \right),
\end{aligned}$$

$$\begin{aligned}
\langle \mathbf{j}^{(f,g)} \rangle = & \sum_{\pm} \int \frac{d\mathbf{p} d\mathbf{k}}{(2\pi)^6} K_{i,j}^{\alpha,\beta}[\mathbf{p}] f_{\pm}(\mathbf{k}) 2e_i A_l^{em} \frac{\hbar^2}{m} \frac{k_j - \frac{p_j}{2}}{\hbar\Omega + i\hbar\eta} \left\{ \left[ \left( \left( \frac{\hbar^2}{m} (\mathbf{k}\mathbf{p} - \frac{p^2}{2}) \mp 2J \right)^2 + i\hbar\eta (\hbar\Omega + i\hbar\eta) \right) \times \right. \right. \\
& (\delta_{\alpha x} \delta_{\beta x} + \delta_{\alpha y} \delta_{\beta y}) \mp (\hbar\Omega + 2i\hbar\eta) \left( \frac{\hbar^2}{m} (\mathbf{k}\mathbf{p} - \frac{p^2}{2}) \mp 2J \right) i (\delta_{\alpha x} \delta_{\beta y} - \delta_{\alpha y} \delta_{\beta x}) \left. \right] \times (A.5) \\
& \frac{((\hbar\Omega + i\hbar\eta) p_l - i\hbar\eta k_l)}{\left( \left( \frac{\hbar^2}{m} (\mathbf{k}\mathbf{p} - \frac{p^2}{2}) \mp 2J \right)^2 + (\hbar\eta)^2 \right) \left( \left( \frac{\hbar^2}{m} (\mathbf{k}\mathbf{p} - \frac{p^2}{2}) \mp 2J \right)^2 - (\hbar\Omega + i\hbar\eta)^2 \right)} + \\
& \left. \frac{\left( \frac{\hbar^4}{m^2} (\mathbf{k}\mathbf{p} - \frac{p^2}{2})^2 + i\hbar\eta (\hbar\Omega + i\hbar\eta) \right) (\hbar\Omega p_l - i\hbar\eta (p_l - k_l))}{\left( \frac{\hbar^4}{m^2} (\mathbf{k}\mathbf{p} - \frac{p^2}{2})^2 + (\hbar\eta)^2 \right) \left( \frac{\hbar^4}{m^2} (\mathbf{k}\mathbf{p} - \frac{p^2}{2})^2 - (\hbar\Omega + i\hbar\eta)^2 \right)} \right\},
\end{aligned}$$

$$\langle \mathbf{j}^{(h)} \rangle = 0, \quad (\text{A.6})$$

$$\langle \mathbf{j}^{(i,j)} \rangle = - \sum_{\pm} \int \frac{d\mathbf{p} d\mathbf{k}}{(2\pi)^6} K_{i,j}^{\alpha,\beta}[\mathbf{p}] f_{\pm}(\mathbf{k}) \mathbf{e}_i A_j^{em} \left\{ \delta_{\alpha z} \delta_{\beta z} \frac{\frac{\hbar^2}{m} p^2}{(\hbar\Omega + i\hbar\eta - \frac{\hbar^2}{m} \mathbf{k}\mathbf{p})^2 - \left(\frac{\hbar^2 p^2}{2m}\right)^2} + \right. \quad (\text{A.7})$$

$$\left. \frac{(\delta_{\alpha x} \delta_{\beta x} + \delta_{\alpha y} \delta_{\beta y}) \frac{\hbar^2}{m} p^2 \pm 2i (\delta_{\alpha x} \delta_{\beta y} - \delta_{\alpha y} \delta_{\beta x}) (\hbar\Omega + i\hbar\eta - \frac{\hbar^2}{m} \mathbf{k}\mathbf{p} \mp 2J)}{(\hbar\Omega + i\hbar\eta - \frac{\hbar^2}{m} \mathbf{k}\mathbf{p} \mp 2J)^2 - \left(\frac{\hbar^2 p^2}{2m}\right)^2} \right\}.$$

- 
- \* eugenk@ipmras.ru
- <sup>1</sup> I. Žutić, J. Fabian, and S. Das Sarma, *Rev. Mod. Phys.* **76**, 323 (2004).
  - <sup>2</sup> G. Tatara, *Physica E* **106**, 208 (2019).
  - <sup>3</sup> R. L. Stamps, S. Breitzkreutz, J. Akerman, A. V. Chumak, Y. Otani, G. E. W. Bauer, J.-U. Thiele, M. Bowen, S. A. Majetich, M. Klaui, I. L. Prejbeanu, B. Dieny, N. M. Dempsey, and B. Hillebrands, *J. Phys. D: Appl. Phys.* **47**, 333001 (2014).
  - <sup>4</sup> W. B. Zeper, H. W. van Kesteren, B. A. J. Jacobs, J. H. M. Spruit, and P. F. Carcia, *Journal of Applied Physics* **69**, 4966 (1991).
  - <sup>5</sup> Z. Kugler, J.-P. Grote, V. Drewello, O. Schebaum, G. Reiss, and A. Thomas, *Journal of Applied Physics* **111**, 07C703 (2012).
  - <sup>6</sup> J. C. Slonczewski, *J. Magn. Magn. Mater.* **159**, L1 (1996).
  - <sup>7</sup> L. Berger, *Phys. Rev. B* **54**, 9353 (1996).
  - <sup>8</sup> Y. Tserkovnyak, A. Brataas, and G. E. W. Bauer, *Phys. Rev. Lett.* **88**, 117601 (2002).
  - <sup>9</sup> A. Brataas, Y. Tserkovnyak, G. E. W. Bauer, and B. I. Halperin, *Phys. Rev. B* **66**, 060404 (2002).
  - <sup>10</sup> Y. B. Bazaliy, B. A. Jones, and S.-C. Zhang, *Phys. Rev. B* **57**, R3213 (1998).
  - <sup>11</sup> S. Zhang and Z. Li, *Phys. Rev. Lett.* **93**, 127204 (2004).
  - <sup>12</sup> Z. Li and S. Zhang, *Phys. Rev. B* **70**, 024417 (2004).
  - <sup>13</sup> A. V. Khvalkovskiy, K. A. Zvezdin, Y. V. Gorbunov, V. Cros, J. Grollier, A. Fert, and A. K. Zvezdin, *Phys. Rev. Lett.* **102**, 067206 (2009).
  - <sup>14</sup> J. Lindner, *Superlattices and Microstructures* **47**, 497 (2010).
  - <sup>15</sup> O. Boule, G. Malinowski, and M. Kläui, *Materials Science and Engineering R* **72**, 159 (2011).
  - <sup>16</sup> J. Shibata, G. Tatara, and H. Kohno, *J. Phys. D: Appl. Phys.* **44**, 384004 (2011).
  - <sup>17</sup> J. A. Katine and E. E. Fullerton, *J. Magn. Magn. Mater.* **320**, 1217 (2008).
  - <sup>18</sup> S. Muhlbauer, B. Binz, F. Jonietz, C. Pfleiderer, A. Rosch, A. Neubauer, R. Georgii, and P. Boni, *Science* **323**, 915 (2009).
  - <sup>19</sup> X. Z. Yu, Y. Onose, N. Kanazawa, J. H. Park, J. H. Han, Y. Matsui, N. Nagaosa, and Y. Tokura, *Nature* **465**, 901 (2010).
  - <sup>20</sup> S. Heinze, K. von Bergmann, M. Menzel, J. Brede, A. Kubetzka, R. Wiesendanger, G. Bihlmayer, and S. Blügel, *Nature Physics* **7**, 713 (2011).
  - <sup>21</sup> N. Nagaosa and Y. Tokura, *Nat. Nano.* **8**, 899 (2013).
  - <sup>22</sup> L. Sun, R. X. Cao, B. F. Miao, Z. Feng, B. You, D. Wu, W. Zhang, A. Hu, and H. F. Ding, *Phys. Rev. Lett.* **110**, 167201 (2013).
  - <sup>23</sup> B. F. Miao, L. Sun, Y. W. Wu, X. D. Tao, X. Xiong, Y. Wen, R. X. Cao, P. Wang, D. Wu, Q. F. Zhan, B. You, J. Du, R. W. Li, and H. F. Ding, *Phys. Rev. B* **90**, 174411 (2014).
  - <sup>24</sup> I. E. Dzyaloshinskii, *Sov. Phys. JETP* **10**, 628 (1960).
  - <sup>25</sup> D. N. Astrov, *Sov. Phys. JETP* **11**, 708 (1960).
  - <sup>26</sup> G. A. Smolenskii and I. E. Chupis, *Sov. Phys. Usp.* **25**, 475 (1982).
  - <sup>27</sup> Y. F. Popov, A. M. Kadomtseva, G. P. Vorob'ev, and A. K. Zvezdin, *Ferroelectrics* **162**, 135 (1994).
  - <sup>28</sup> A. P. Pyatakov and A. K. Zvezdin, *Physics-Uspexhi* **55**, 557 (2012).
  - <sup>29</sup> H. Katsura, N. Nagaosa, and A. V. Balatsky, *Phys. Rev. Lett.* **95**, 057205 (2005).
  - <sup>30</sup> P. Bruno and V. K. Dugaev, *Phys. Rev. B* **72**, 241302 (2005).
  - <sup>31</sup> I. S. Veshchunov, S. V. Mironov, W. Magrini, V. S. Stolyarov, A. N. Rossolenko, V. A. Skidanov, J.-B. Trebbia, A. I. Buzdin, P. Tamarat, and B. Lounis, *Phys. Rev. Lett.* **115**, 027601 (2015).
  - <sup>32</sup> A. S. Logginov, G. A. Meshkov, A. V. Nikolaev, E. P. Nikolaeva, A. P. Pyatakov, and A. K. Zvezdin, *Applied Physics Letters* **93**, 182510 (2008).
  - <sup>33</sup> D. P. Kulikova, T. T. Gareev, E. P. Nikolaeva, T. B. Kosykh, A. V. Nikolaev, Z. A. Pyatakova, A. K. Zvezdin, and A. P. Pyatakov, *physica status solidi (RRL) Rapid Research Letters* **12**, 1800066 (2018).
  - <sup>34</sup> E. Sonin, *Advances in Physics* **59**, 181 (2010).
  - <sup>35</sup> M. Chshiev, A. Manchon, A. Kalitsov, N. Ryzhanova, A. Vedyayev, N. Strelkov, W. H. Butler, and B. Dieny, *Phys. Rev. B* **92**, 104422 (2015).
  - <sup>36</sup> J. König, M. C. Bønsager, and A. H. MacDonald, *Phys. Rev. Lett.* **87**, 187202 (2001).
  - <sup>37</sup> W. Chen, P. Horsch, and D. Manske, *Phys. Rev. B* **89**, 064427 (2014).
  - <sup>38</sup> Y. G. Shen and Z. H. Yang, *EPL (Europhysics Letters)* **78**, 17003 (2007).
  - <sup>39</sup> J. Wang and K. S. Chan, *Journal of Physics: Condensed Matter* **19**, 236215 (2007).
  - <sup>40</sup> B. Wang, J. Peng, D. Y. Xing, and J. Wang, *Phys. Rev. Lett.* **95**, 086608 (2005).
  - <sup>41</sup> J. Wang and K. S. Chan, *Phys. Rev. B* **74**, 035342 (2006).
  - <sup>42</sup> J. Wang, B.-F. Zhu, and R.-B. Liu, *Phys. Rev. Lett.* **104**,

- 256601 (2010).
- <sup>43</sup> L. K. Werake and H. Zhao, *Nature Phys.* **6**, 875 (2010).
- <sup>44</sup> E. A. Karashtin and A. A. Fraerman, *J. Phys. Condens. Matter* **30**, 165801 (2018).
- <sup>45</sup> E. A. Karashtin, *Phys. Solid State* **59**, 2189 (2017).
- <sup>46</sup> E. A. Karashtin, *JETP Letters* **108**, 97 (2018).
- <sup>47</sup> L. D. Landau and E. M. Lifshitz, *Course of Theoretical Physics, Vol. 8: Electrodynamics of Continuous Media* (Butterworth - Heinemann, Oxford, 1984).
- <sup>48</sup> E. I. Rashba, *Fiz.Tverd.Tela.Sov.Phys.-Solid State* **2**, 1224 (1960).
- <sup>49</sup> H. Haug and A.-P. Jauho, *Quantum Kinetics in Transport and Optics of Semiconductors* (Springer-Verlag, Berlin, Heidelberg, New York, 2008).
- <sup>50</sup> O. G. Udalov, M. V. Sapozhnikov, E. A. Karashtin, B. A. Gribkov, S. A. Gusev, E. V. Skorohodov, V. V. Rogov, A. Y. Klimov, and A. A. Fraerman, *Phys. Rev. B* **86**, 094416 (2012).
- <sup>51</sup> E. A. Karashtin, *Phys. Rev. B* **87**, 094418 (2013).
- <sup>52</sup> I. A. Kolmychek, V. L. Krutyanskiy, T. V. Murzina, M. V. Sapozhnikov, E. A. Karashtin, V. V. Rogov, and A. A. Fraerman, *J. Opt. Soc. Am. B* **32**, 331 (2015).
- <sup>53</sup> J. Shibata, A. Takeuchi, H. Kohno, and G. Tatara, *Journal of Applied Physics* **123**, 063902 (2018), <https://doi.org/10.1063/1.5011130>.
- <sup>54</sup> M. Calvo, *Phys. Rev. B* **19**, 5507 (1979).
- <sup>55</sup> E. A. Karashtin and O. G. Udalov, *J. Exp. Theor. Phys.* **113**, 992 (2011).
- <sup>56</sup> A. N. Bogdanov and U. K. Röbber, *Phys. Rev. Lett.* **87**, 037203 (2001).
- <sup>57</sup> A. K. Zvezdin, *Bulletin of the Lebedev Physics Institute* **4**, 7 (2002).
- <sup>58</sup> K.-W. Kim, H.-W. Lee, K.-J. Lee, and M. D. Stiles, *Phys. Rev. Lett.* **111**, 216601 (2013).
- <sup>59</sup> K. M. D. Hals and K. Everschor-Sitte, *Phys. Rev. Lett.* **119**, 127203 (2017).
- <sup>60</sup> A. Finco, L. Rózsa, P.-J. Hsu, A. Kubetzka, E. Vedmedenko, K. von Bergmann, and R. Wiesendanger, *Phys. Rev. Lett.* **119**, 037202 (2017).
- <sup>61</sup> A. Sparavigna, A. Strigazzi, and A. Zvezdin, *Phys. Rev. B* **50**, 2953 (1994).
- <sup>62</sup> C. Tabares-Munos, J. P. Rivera, A. Bezinges, A. Mounier, and H. Schmid, *Jpn. J. Appl. Phys.* **24**, 1051 (1985).
- <sup>63</sup> A. K. Zvezdin and A. P. Pyatakov, *EPL (Europhysics Letters)* **99**, 57003 (2012).
- <sup>64</sup> K.-W. Kim, H.-W. Lee, K.-J. Lee, and M. D. Stiles, *Phys. Rev. Lett.* **111**, 216601 (2013).